Pervasive aqueous alteration in the early Solar System revealed by potassium isotopic variations in Ryugu samples and carbonaceous chondrites

Yan Hu, Frédéric Moynier, Wei Dai, Marine Paquet, Tetsuya Yokoyama, Yoshinari Abe, Jérôme Aléon, Conel M. O'D. Alexander, Sachiko Amari, Yuri Amelin, et al.

Version of Record: https://www.sciencedirect.com/science/article/pii/S0019103523004633
Manuscript_07df0645701beae8fe78d0245b6148ac

Pervasive aqueous alteration in the early Solar System revealed by potassium isotopic variations in Ryugu samples and carbonaceous chondrites

Yan Hu[1,*], Frédéric Moynier[1,*], Wei Dai[1], Marine Paquet[1], Tetsuya Yokoyama[2], Yoshinari Abe[3], Jérôme Aléon[4], Conel M. O'D. Alexander[5], Sachiko Amari[6,7], Yuri Amelin[8], Ken-ichi Bajo[9], Martin Bizzarro[10,1], Audrey Bouvier[11], Richard W. Carlson[5], Marc Chaussidon[1], Byeon-Gak Choi[12], Nicolas Dauphas[13], Andrew M. Davis[13], Tommaso Di Rocco[14], Wataru Fujiya[15], Ryota Fukai[16], Ikshu Gautam[2], Makiko K. Haba[2], Yuki Hibiya[17], Hiroshi Hidaka[18], Hisashi Homma[19], Peter Hoppe[20], Gary R. Huss[21], Kiyohiro Ichida[22], Tsuyoshi Iizuka[23], Trevor R. Ireland[24], Akira Ishikawa[2], Shoichi Itoh[25], Noriyuki Kawasaki[9], Noriko T. Kita[26], Koki Kitajima[26], Thorsten Kleine[27], Shintaro Komatani[22], Alexander N. Krot[21], Ming-Chang Liu[28], Yuki Masuda[2], Mayu Morita[22], Kazuko Motomura[29], Izumi Nakai[30], Kazuhide Nagashima[21], David Nesvorný[31], Ann Nguyen[32], Larry Nittler[5,33], Morihiko Onose[22], Andreas Pack[14], Changkun Park[34], Laurette Piani[35], Liping Qin[36], Sara S. Russell[37], Naoya Sakamoto[38], Maria Schönbächler[39], Lauren Tafla[28], Haolan Tang[28,36], Kentaro Terada[40], Yasuko Terada[41], Tomohiro Usui[16], Sohei Wada[9], Meenakshi Wadhwa[33], Richard J. Walker[42], Katsuyuki Yamashita[43], Qing-Zhu Yin[44], Shigekazu Yoneda[45], Edward D. Young[28], Hiroharu Yui[46], Ai-Cheng Zhang[47], Tomoki Nakamura[48], Hiroshi Naraoka[49], Takaaki Noguchi[25], Ryuji Okazaki[49], Kanako Sakamoto[16], Hikaru Yabuta[50], Masanao Abe[16], Akiko Miyazaki[16], Aiko Nakato[16], Masahiro Nishimura[16], Tatsuaki Okada[16], Toru Yada[16], Kasumi Yogata[16], Satoru Nakazawa[16], Takanao Saiki[16], Satoshi Tanaka[16], Fuyuto Terui[51], Yuichi Tsuda[16], Sei-ichiro Watanabe[18], Makoto Yoshikawa[16], Shogo Tachibana[52], Hisayoshi Yurimoto[9]

Affiliations

[1]Université Paris Cité, Institut de Physique du Globe de Paris, CNRS, 75005 Paris, France.
[2]Department of Earth and Planetary Sciences, Tokyo Institute of Technology, Tokyo 152-8551, Japan.
[3]Graduate School of Engineering, Tokyo Denki University, Tokyo 120-8551, Japan.
[4]Institut de Minéralogie, de Physique des Matériaux et de Cosmochimie, Sorbonne Université, Museum National d'Histoire Naturelle, CNRS UMR 7590, IRD, 75005 Paris, France.
[5]Earth and Planets Laboratory, Carnegie Institution for Science, Washington, DC, 20015, USA.
[6]McDonnell Center for the Space Sciences and Physics Department, Washington University, St. Louis, MO 63130, USA.
[7]Geochemical Research Center, The University of Tokyo, Tokyo, 113-0033, Japan
[8]Korea Basic Science Institute, Ochang, Cheongwon, Cheongju, Chungbuk 28119, Republic of Korea
[9]Department of Natural History Sciences, Hokkaido University, Sapporo 001-0021, Japan.
[10]Centre for Star and Planet Formation, GLOBE Institute, University of Copenhagen, Copenhagen, K 1350, Denmark.
[11]Bayerisches Geoinstitut, Universität Bayreuth, Bayreuth 95447, Germany.
[12]Department of Earth Science Education, Seoul National University, Seoul 08826, Republic of Korea.
[13]Department of the Geophysical Sciences and Enrico Fermi Institute, The University of Chicago, 5734 South Ellis Avenue, Chicago 60637, USA.

[14]Faculty of Geosciences and Geography, University of Göttingen, Göttingen, D-37077, Germany.
[15]Faculty of Science, Ibaraki University, Mito 310-8512, Japan.
[16]ISAS/JSEC, JAXA, Sagamihara 252-5210, Japan.
[17]Research Center for Advanced Science and Technology, The University of Tokyo, Tokyo 153-8904, Japan.
[18]Department of Earth and Planetary Sciences, Nagoya University, Nagoya 464-8601, Japan.
[19]Osaka Application Laboratory, SBUWDX, Rigaku Corporation, Osaka 569-1146, Japan.
[20]Max Planck Institute for Chemistry, Mainz 55128, Germany.
[21]Hawai‘i Institute of Geophysics and Planetology, University of Hawai‘i at Mānoa, Honolulu, HI 96822, USA.
[22]Analytical Technology, Horiba Techno Service Co., Ltd., Kyoto 601-8125, Japan.
[23]Department of Earth and Planetary Science, The University of Tokyo, Tokyo 113-0033, Japan.
[24]School of Earth and Environmental Sciences, The University of Queensland, St Lucia QLD 4072, Australia.
[25]Division of Earth and Planetary Sciences, Kyoto University, Kyoto 606-8502, Japan.
[26]Department of Geoscience, University of Wisconsin-Madison, Madison, WI 53706, USA.
[27]Max Planck Institute for Solar System Research, 37077 Göttingen, Germany.
[28]Department of Earth, Planetary, and Space Sciences, UCLA, Los Angeles, CA 90095, USA.
[29]Thermal Analysis, Rigaku Corporation, Tokyo 196-8666, Japan.
[30]Department of Applied Chemistry, Tokyo University of Science, Tokyo 162-8601, Japan.
[31]Department of Space Studies, Southwest Research Institute, Boulder, CO 80302, USA.
[32]Astromaterials Research and Exploration Science, NASA Johnson Space Center, Houston, TX 77058, USA.
[33]School of Earth and Space Exploration, Arizona State University, Tempe, AZ 85281, USA.
[34]Earth-System Sciences, Korea Polar Research Institute, Incheon 21990, Korea.
[35]Centre de Recherches Pétrographiques et Géochimiques, CNRS - Université de Lorraine, 54500 Nancy, France.
[36]CAS Key Laboratory of Crust-Mantle Materials and Environments, University of Science and Technology of China, School of Earth and Space Sciences, Anhui 230026, China.
[37]Department of Earth Sciences, Natural History Museum, London, SW7 5BD, UK.
[38]Isotope Imaging Laboratory, Creative Research Institution, Hokkaido University, Sapporo 001-0021, Japan.
[39]Institute for Geochemistry and Petrology, Department of Earth Sciences, ETH Zurich, 8092 Zurich, Switzerland.
[40]Department of Earth and Space Science, Osaka University, Osaka 560-0043, Japan.
[41]Spectroscopy and Imaging, Japan Synchrotron Radiation Research Institute, Hyogo 679-5198 Japan.
[42]Department of Geology, University of Maryland, College Park, MD 20742, USA.
[43]Graduate School of Natural Science and Technology, Okayama University, Okayama 700-8530, Japan.
[44]Department of Earth and Planetary Sciences, University of California, Davis, CA 95616, USA.
[45]Department of Science and Engineering, National Museum of Nature and Science, Tsukuba 305-0005, Japan.
[46]Department of Chemistry, Tokyo University of Science, Tokyo 162-8601, Japan.
[47]School of Earth Sciences and Engineering, Nanjing University, Nanjing 210023, China.
[48]Department of Earth Science, Tohoku University, Sendai, 980-8578, Japan.

[49]Department of Earth and Planetary Sciences, Kyushu University, Fukuoka 819-0395, Japan.
[50]Earth and Planetary Systems Science Program, Hiroshima University, Higashi-Hiroshima 739-8526, Japan.
[51]Kanagawa Institute of Technology, Atsugi 243-0292, Japan.
[52]UTokyo Organization for Planetary and Space Science, The University of Tokyo, Tokyo 113-0033, Japan.

Abstract: 233 words

Main text: 4512 words

Figures: 3

Table: 1

Submit to ***Icarus***

Revised version

(November, 2023)

*Corresponding authors:

Email: yanhu@ipgp.fr; moynier@ipgp.fr

Abstract

C-type asteroids are the presumed home to carbonaceous chondrites, some of which contain abundant life-forming volatiles and organics. For the first time, samples from a C-type asteroid (162173 Ryugu) were successfully returned to Earth by JAXA's Hayabusa2 mission. These pristine samples, uncontaminated by the terrestrial environment, allow a direct comparison with carbonaceous chondrites. This study reports the stable K isotopic compositions (expressed as $\delta^{41}K$) of Ryugu samples and seven carbonaceous chondrites to constrain the origin of K isotopic variations in the early Solar System. Three aliquots of Ryugu particles collected at two touchdown sites have identical $\delta^{41}K$ values, averaged at −0.194 ± 0.038‰ (2SD). The K isotopic composition of Ryugu falls within the range of $\delta^{41}K$ values measured on representative CI chondrites, and together, they define an average $\delta^{41}K$ value of −0.185 ± 0.078‰ (2SE), which provides the current best estimate of the K isotopic composition of the bulk Solar System. Samples of CI chondrites with $\delta^{41}K$ values that deviate from this range likely reflect terrestrial contaminations or compositional heterogeneities at sampled sizes. In addition to CI chondrites, substantial K isotopic variability is observed in other carbonaceous chondrites and within individual chondritic groups, with $\delta^{41}K$ values inversely correlated with K abundances in many cases. These observations indicate widespread fluid activity occurred in chondrite parent bodies, which significantly altered the original K abundances and isotopic compositions of chondrules and matrices established at their accretion.

Keywords: Asteroid Ryugu; Hayabusa2 mission; Carbonaceous chondrites; Stable potassium isotopes; Aqueous alteration

1 Introduction

Primitive asteroids accreted varying amounts of ice that melted to water-rich fluids due to heat released from the radioactive decay of short-lived nuclides (e.g., ^{26}Al, McSween et al., 2002) and possibly from impacts (Rubin, 2012). Consequently, fluid activity is believed to have been pervasive in the early history of planetesimal and planet development (Brearley, 2006; Brearley, 2014; Clayton, 1993; Zolensky and McSween, 1988). Potassium (K) is a fluid-mobile, large-ion lithophile element that resides primarily in chondrule mesostasis and fine-grained matrix in carbonaceous asteroids. These components react readily with aqueous fluids, leading to redistribution of K^+ and its isotopes. In addition, K is a moderately volatile metal that is variably depleted in carbonaceous chondrites and terrestrial planetary bodies. Because both volatility-driven depletion and fluid-rock interaction can lead to mass-dependent fractionations between the two stable K isotopes (i.e., ^{39}K and ^{41}K), it is essential to understand how these processes affect δ^{41}K variations in meteorites to facilitate the interpretation of K isotopic signatures of planetary materials.

Carbonaceous Ivuna-type (CI) chondrites are the chemically most primitive meteorites and have been widely used to infer the isotopic composition of the bulk Solar System (Palme et al., 2014). Despite their primitive bulk composition, CI chondrites underwent near-complete aqueous alteration of anhydrous precursors to secondary mineral assemblages dominated by phyllosilicates (e.g., Tomeoka and Buseck, 1988) and display significant small-scale chemical heterogeneities (e.g., Barrat et al., 2012; Morlok et al., 2006; Palme and Zipfel, 2022). Because CI chondrites are limited in numbers and masses, previous K isotopic analyses focused on the largest witnessed fall (Orgueil, 14 kg) and the CI-type specimen (Ivuna, 0.7 kg). Earlier analyses of Orgueil returned a δ^{41}K value (−0.534 ± 0.097‰, 2SE) that is similar to the bulk Silicate Earth (Wang and Jacobsen, 2016); however, this sample shows elemental enrichments (e.g., K, Rb, Ba, Th, and U) that indicate significant contamination on Earth (Ku and Jacobsen, 2020). Reported δ^{41}K values of other Orgueil samples vary between −0.290‰ and −0.039‰ (Hu et al., 2022, 2023; Koefoed et al., 2022, 2023; Ku and Jacobsen, 2020; Nie et al., 2021), with the six distinct stones reported by Koefoed et al. (2022; 2023) displaying more uniform δ^{41}K values ranging from −0.290‰ to −0.170‰. However, while Koefoed et al. (2023) reported a similar δ^{41}K value of −0.180 ± 0.060‰ for Ivuna, a markedly lower value of −0.460 ± 0.046‰ was reported for another Ivuna sample with a similar K abundance (Nie et al., 2021). The cause of

this intra-group difference remains unclear. It may reflect an unrepresentative sampling of the bulk composition due to sample heterogeneity caused by aqueous alteration in the parent body(s) of the CI chondrites or remobilization of K in terrestrial environments. A better-defined K isotopic composition of CI chondrites is critical for constraining the bulk composition of the Solar System.

In December 2020, JAXA's Hayabusa2 mission returned the first samples from the carbonaceous asteroid 162173 Ryugu, which had not been exposed to terrestrial environments prior to laboratory analysis. These samples contain abundant organic material plausibly inherited from the protosolar nebula and/or the interstellar medium, which attests to their primitive nature (Nakamura et al., 2022; Pilorget et al., 2022). Furthermore, chemical and isotopic analyses suggest that Ryugu has a similar bulk composition to CI chondrites (Hopp et al., 2022; Moynier et al., 2022; Nakamura et al., 2022; Paquet et al., 2022; Yokoyama et al., 2022). In particular, the Ryugu samples do not contain chondrules or refractory inclusions (Pilorget et al., 2022; Yokoyama et al., 2022) and display no depletion of volatile metals relative to the solar photosphere (Yokoyama et al., 2022), which are essential features of CI chondrites. Therefore, the Ryugu samples are a direct asteroidal analogue to CI chondrites. Here, we report the K isotopic compositions of three aliquots of Ryugu particles collected from two touchdown sites and seven carbonaceous chondrites measured with the Nu Sapphire collision-cell multi-collector inductively-coupled plasma mass spectrometer (CC-MC-ICP-MS) to further constrain the pristine composition of CI chondrites and the origin of K isotopic variation in the Solar System.

2 Samples and methods

2.1 Sample description and pre-chemistry preparation

Ryugu formed as a rubble-pile asteroid (approximately 1 km in diameter) reaccumulated from the shattered debris of a larger parent body (Sugita et al., 2019); therefore, Ryugu likely sampled rock fragments from all depths of its parent body. The Hayabusa2 mission retrieved 5.4 g of pebbles and sands at two locations on Ryugu (Tachibana et al., 2022; Yada et al., 2022). Around 3 g of surface material was collected from the touchdown site 1 and stored in Chamber A (Morota et al., 2020). The second landing targeted at collecting impact ejecta from a ~ 15-m diameter crater artificially made by the onboard Small Carry-on Impactor (SCI) (Arakawa et al.,

2020). Around 2 g of samples containing subsurface material was collected from the touchdown site 2 and stored in Chamber C. Samples collected from these two sites are considered representative of the compositionally homogeneous Ryugu surface based on their consistent spectral features and physical properties (color, shape, surface morphology, and structure) with onboard measurements made by the spacecraft (Kitazato et al., 2019; Nakamura et al., 2022; Pilorget et al., 2022; Tachibana et al., 2022).

Three aliquots of Ryugu particles were analyzed for K isotopes. Sample A0106 is from Chamber A, while samples C0107 and C0108 are from Chamber C. Preliminary sample treatment has been performed at the Tokyo Institute of Technology (Tokyo Tech). Samples A0106 and C0107 were first treated to extract soluble organic matter (Naraoka et al., 2023). Then, together with C0108, they were dissolved in pre-cleaned perfluoroalkoxy (PFA) vials in a mixture of concentrated HF and HNO_3, as described in Yokoyama et al. (2022). All three Ryugu samples were first processed to separate the Zn fractions from other constituent elements in the samples (Paquet et al., 2022). This was followed by a three-step sequential chemical separation procedure for the isotopic measurements of Fe (Hopp et al., 2022), Ti, and Cr (Yokoyama et al., 2022), after which we obtained a fraction containing mainly K, Mg, and Ni. Aliquots of the K-Mg-Ni fraction for the Ryugu samples were transferred to the Institut de Physique du Globe de Paris (IPGP) for K isotopic analyses. The amounts of K finally obtained from the three Ryugu samples ranged from 1365 to 2867 ng. To verify whether the multi-stage chemical separation fractionated the K isotopes, the K-Mg-Ni fractions of three carbonaceous chondrites, including Tarda (C2-ungrouped), Tagish Lake (C2-ungrouped), and Allende (CV3), which were subjected to the same processing as the Ryugu samples at Tokyo Tech, were chemically purified for K isotopic analyses at IPGP.

We also analyzed four geostandards (BIR, BCR-2, AGV-2, and seawater) and seven in-house carbonaceous chondrites at IPGP to examine possible sample heterogeneity and to compare with the K isotopic compositions of the Ryugu samples. The additional chondrite samples were: Orgueil (CI1), Tagish Lake (C2-ungrouped), Tarda (C2-ungrouped), Cold Bokkeveld (CM2), Murchison (CM2), Lancé (CO3.5), and Allende (CV3). At IPGP, approximately 8-15 mg of the sample powders were dissolved in Savillex screw-top PFA beakers using sequential addition of concentrated HF-HNO_3 (3:1), HCl-HNO_3 (3:1), and HNO_3. The dissolved sample solutions were refluxed with and redissolved in 0.5 mol/L HNO_3.

2.2 Potassium purification and isotope measurement

Potassium was isolated from other elements by cation-exchange chromatography described in Xu et al. (2019). Two mL of Bio-Rad AG 50W-X8 cation exchange resin (200-400 mesh) was filled into pre-cleaned Bio-Rad Poly-Prep columns. The resin was cleaned by three passes with 6 mol/L HCl, one pass with 6 mol/L HNO_3, and one pass with 1 mol/L HNO_3. Each acid pass was rinsed with 10 mL of Milli-Q deionized water. The resin was then conditioned with 10 mL of 0.5 mol/L HNO_3. Dissolved sample solutions were loaded onto the resin in 1 mL of 0.5 mol/L HNO_3. A volume of 13 mL of 0.5 mol/L HNO_3 was passed through the column, and the K fraction was collected in the subsequent 22 mL of the same acid. The sample solutions were passed through the column four times. This chromatography protocol provides a K yield greater than 99.3% and effectively separates matrix elements from the K fractions, as have been evaluated in previous studies (Xu et al., 2019; Hu et al., 2022). The K blank introduced by each pass of column chemistry is ~ 0.2 ng, and the whole-procedure K blank varies between 3.7 ng and 6.2 ng (Hu et al., 2022), which is insignificant (< 1%) compared to the amounts of K in processed samples.

Potassium isotopic analyses followed the protocol described by Moynier et al. (2021). Purified K fractions were diluted in 0.5 mol/L HNO_3 to have K concentrations between 60 ppb and 70 ppb. They were introduced into the mass spectrometer using an Apex Omega desolvation nebulizer system fitted with a 100 µL/min nebulizer. The ion beam was first decelerated to enter a hexapole collision cell to remove interfering species (e.g., $^{40}ArH^+$ on $^{41}K^+$), and the $^{41}K^+$ and $^{39}K^+$ ion beams were accelerated and directed through the magnet to the Faraday collectors. Each analysis consisted of a 90-second transfer time, a 60-second zero measurement in a blank solution, and 50 cycles of sample measurement with 5-second integration. A 150-second wash was performed between analyses. Each sample solution was paired with a standard solution diluted to the same K concentration (to within 2%). Standard and sample solutions were analyzed alternatively during a sequence to correct for instrumental mass bias. Potassium isotopic data are reported as the average of repeated analyses (4 to 8 times) relative to NIST SRM 3141a in delta notation:

$$\delta^{41}\mathrm{K}\ (‰) = \left\{ \frac{\left(^{41}\mathrm{K}/^{39}\mathrm{K}\right)_{\mathrm{sample}}}{\left(^{41}\mathrm{K}/^{39}\mathrm{K}\right)_{\mathrm{NIST\ SRM\ 3141a}}} - 1 \right\} \times 1000$$

Analytical uncertainties are reported as 2SD (standard deviation) and 95% c.i. (confidence interval) in Table 1 and Table S1. In the following sections, analytical uncertainty used for individual sample is 95% c.i. and that used for group average is 2SD unless stated otherwise.

3 Results and discussions

3.1 Analytical accuracy

We first evaluate the accuracy of our analyses by comparing the δ^{41}K values of representative terrestrial standards and chondrites from analyses in this study to previous results. The δ^{41}K values of basalt BIR (−0.418 ± 0.031‰) and BCR-2 (−0.426 ± 0.030‰), andesite AGV-2 (−0.455 ± 0.030‰), and Pacific seawater (0.126 ± 0.028‰) analyzed during the course of this study agree well with published results (Chen et al., 2019; Hille et al., 2019; Hu et al., 2018; Moynier et al., 2021; Xu et al., 2019). In addition, Orgueil (−0.081 ± 0.066‰), Murchison (−0.250 ± 0.043‰), Allende (−0.169 ± 0.030‰), Cold Bokkeveld (−0.267 ± 0.035‰), and Lancé (−0.382 ± 0.040‰) processed and analyzed in this study yielded consistent values with our previous analyses (Hu et al., 2022; Hu et al., 2023). This consistency confirms the accuracy of our analyses.

We then evaluate whether the multi-stage chemical separation procedures performed at Tokyo Tech affected the isotopic compositions of K in the samples. For Tagish Lake, the K extracted from the K-Mg-Ni fraction has a δ^{41}K value of −0.180 ± 0.049‰, which is indistinguishable from the values obtained from two new dissolutions of separate pieces of this meteorite from Tokyo Tech (−0.215 ± 0.043‰) and IPGP (−0.215 ± 0.032‰). Likewise, the K purified from the K-Mg-Ni fraction of Tarda (−0.223 ± 0.037‰) is isotopically identical to that purified from a separate piece of this meteorite at IPGP (−0.205 ± 0.024‰). This similarity in δ^{41}K values suggests that the preliminary chemical processing performed at Tokyo Tech affected K negligibly. In support of this inference, the anion resin used to separate Zn from other constituent elements in the samples should not retain any K^+, which would be eluted from the resin. Therefore, it is reasonable to assume that the δ^{41}K values of K extracted from the K-Mg-Ni fraction of the three Ryugu samples are representative of these samples. While the K-Mg-Ni

fraction of Allende (−0.292 ± 0.044‰) is isotopically different from our in-house Allende sample (−0.169 ± 0.030‰), the δ^{41}K values of both samples fall within the reported range from −0.620 ± 0.050‰ to −0.082 ± 0.030‰ (Bloom et al., 2020; Ku and Jacobsen, 2020; Nie et al., 2021; Jiang et al., 2021; Hu et al., 2023; Koefoed et al., 2023). The discrepancy between the two Allende samples thus likely reflects sample heterogeneity.

3.2 Stable K isotopic compositions of CI chondrites and the bulk Solar System

The three Ryugu samples have K abundances that are comparable to those of the CI chondrites (Fig. 1A). In addition, they display consistent δ^{41}K values (Fig. 1B), with no significant differences between the samples collected from the touchdown site 1 (Chamber A sample A0106 = −0.172 ± 0.039‰) and the touchdown site 2 (Chamber C samples C0107 = −0.204 ± 0.048‰ and C0108 = −0.207 ± 0.055‰). Furthermore, the two samples from Chamber C have essentially identical δ^{41}K values, indicating that the extraction of soluble organic matter from samples C0107 and A0106 prior to K separation did not affect their K isotopic compositions. The three Ryugu samples yield an average δ^{41}K value of −0.194 ± 0.038‰ (2SD), which falls within the range of CI chondrites (Fig. 1B). This result is consistent with previous observations of CI-like isotopic compositions of Ryugu for the moderately volatile elements Zn and Cu (Paquet et al., 2022) and the more refractory elements Fe, Cr, Ti, and Ca (Hopp et al., 2022; Moynier et al., 2022; Yokoyama et al., 2022). The stable K isotope ratios thus further strengthen the compositional links between Ryugu and CI chondrites.

The new data from Ryugu samples provide critical constraints on the K isotopic composition of the bulk Solar System, which can otherwise only be inferred from CI chondrites. Previous analyses of CI chondrites show highly variable δ^{41}K values from −0.534‰ to −0.039‰, covering almost the entire variation measured in carbonaceous chondrites (Hu et al., 2022, 2023; Koefoed et al., 2022, 2023; Ku and Jacobsen, 2020; Nie et al., 2021; Wang and Jacobsen, 2016). Ku and Jacobsen (2020) found that the lowest δ^{41}K values were measured for a piece of Orgueil contaminated with 8% continental crust material, resulting in its substantially higher K abundance and lower δ^{41}K value than other Orgueil samples (Fig. 1). In contrast, the 11 other Orgueil samples show a limited K isotopic range from −0.290‰ to −0.039‰, with six stones reported by Koefoed et al. (2023) having similar values between −0.290‰ and −0.170‰ (Fig.

1B). All these analyses together give an average δ^{41}K value of −0.182 ± 0.148‰ (2SD), suggesting a largely homogeneous K isotopic composition in Orgueil. The small variability between different Orgueil samples could be due to aqueous redistribution, as suggested by a slightly negative correlation between the δ^{41}K value and K abundance (Fig. 1B).

Unlike Orgueil, however, there is a large discrepancy in the δ^{41}K values reported for two separate analyses of the CI-type specimen Ivuna. The lower value of −0.460 ± 0.046‰ does not appear to reflect terrestrial contamination because this Ivuna sample has a normal K abundance (458 ppm, Nie et al., 2021) as the uncontaminated Orgueil samples and the other Ivuna sample, which has a δ^{41}K value (−0.180 ± 0.060‰, Koefoed et al., 2023) similar to the Orgueil average calculated above (Fig. 1B). Given that this lower Ivuna value is significantly lower than those of the Ryugu samples, it likely reflects an unrepresentative sampling of the bulk Ivuna composition. This inference is supported by the heterogenous distribution of soluble elements in CI chondrites, in particular for Ivuna (Barrat et al., 2012; Brearley, 2006; Morlok et al., 2006; Palme and Zipfel, 2022) (Fig. 1A). Excluding the anomalous Ivuna value, representative averages of Ryugu (−0.194 ± 0.022‰, 2SE) and Orgueil (−0.182 ± 0.045‰, 2SE) and a single Ivuna value (−0.180 ± 0.060‰, 2SE, Koefoed et al., 2023) define an arithmetic mean of −0.185 ± 0.078‰ (2SE). This δ^{41}K mean agrees with the recently proposed average CI value of −0.21 ± 0.05‰ (Koefoed et al., 2023) calculated by averaging 15 published CI data (including the anomalous Ivuna value). The agreement between the two estimates further supports a relatively homogeneous K isotopic composition of the bulk Solar System.

3.3 Origin of K isotopic variations in carbonaceous chondrites

A well-established average δ^{41}K value of CI chondrites is an important reference for understanding the origin of K isotopic variations among different carbonaceous chondritic groups. This is because CI chondrites are generally used to approximate the isotopic composition of the matrix component in carbonaceous chondrites (e.g., Alexander, 2005; Braukmüller et al., 2018), and a robust δ^{41}K value for CI chondrites is critical for explaining the K isotopic variations in carbonaceous chondrites (Bloom et al., 2020; Ku and Jacobsen, 2020; Nie et al., 2021; Hu et al., 2022, 2023; Koefoed et al., 2022, 2023). The average δ^{41}K values established for CI chondrites and Ryugu samples in this study agree with each other within uncertainty (Fig. 2).

Their $\delta^{41}K$ values also overlap within uncertainty with those of the two ungrouped C2 chondrites (Tagish Lake and Tarda), which contain the second-highest matrix volume among carbonaceous chondrites (Fig. 2). These observations indicate that the CI-like matrix in carbonaceous chondrites is largely homogeneous in $\delta^{41}K$.

Compared with CI chondrites and Ryugu samples, carbonaceous chondrites from the CM (Murchison), CO (Lancé), and CV (Allende) groups are variably depleted in the heavier K isotope, and their $\delta^{41}K$ values correlate positively with the $\delta^{66}Zn$ and $\delta^{65}Cu$ values (Fig. 2). Positive correlations are also evident between $\delta^{41}K$ with isotopes of other MVEs, including Rb, Sn, and Te, in a larger dataset of carbonaceous chondrites (Hu et al., 2023; Koefoed et al., 2023; Nie et al., 2021). In addition, a broad negative correlation between $\delta^{41}K$ and 1/[K] was reported by Nie et al. (2021) for seven carbonaceous chondrites, from which they extrapolated a $\delta^{41}K$ value of −0.33 ± 0.12‰ for the chondrule component and of 0.04 ± 0.08‰ for the matrix component. These systematic correlations reflect the early formation of two nebular reservoirs, with a volatile-depleted refractory component (e.g., chondrules) carrying the light isotopic signatures, and a CI-like reservoir with the heaviest isotopic compositions, as initially proposed by Luck et al. (2005; 2003). When all available data are considered, there is a coinciding increase in $\delta^{41}K$ with water content (as a proxy for matrix content) and a decrease in $\delta^{41}K$ with chondrule content in chondrites, further substantiating the role of chondrules as the carriers of K depletion and low-$\delta^{41}K$ signature in chondrites (Hu et al., 2023). Therefore, the inter-group K isotopic variations in carbonaceous chondrites primarily reflect variable mixing between the two main K hosts, i.e., chondrules and the matrix, accreted by the parent bodies of carbonaceous chondrites.

3.4 Potassium isotopic evidence for widespread aqueous alteration in chondrite parent bodies

Although chondrule-matrix mixing could explain the inter-group $\delta^{41}K$ variation among carbonaceous chondrites, the significant variability within individual chondrites remains perplexing. In addition to the anomalously low $\delta^{41}K$ value reported for Ivuna, substantial variability has also been documented for Allende and Murchison. Our in-house Allende sample has a higher $\delta^{41}K$ value (−0.169 ± 0.030‰) than the sample provided by the Smithsonian

Museum (−0.292 ± 0.044‰), while they both fall within the previously reported range of −0.620‰ to −0.080‰ for Allende (Bloom et al., 2020; Jiang et al., 2021a; Koefoed et al., 2023; Ku and Jacobsen, 2020; Nie et al., 2021). Furthermore, the Allende sample provided by the Smithsonian Museum is an aliquot from a large batch of homogenized powder, and its $\delta^{41}K$ value is in the middle of the reported range. Our Murchison sample also has a $\delta^{41}K$ value (−0.250 ± 0.043‰) that is in the middle of the previously reported range for Murchison (−0.410‰ to −0.101‰, Jiang et al., 2021b; Koefoed et al., 2023; Ku and Jacobsen, 2020; Nie et al., 2021).

To identify the cause of intra-chondrite isotopic variability, we compare the two sets of $\delta^{41}K$ vs. $\delta^{87}Rb$ data obtained from IPGP and those reported in Nie et al. (2021), respectively, for four carbonaceous chondrites. While the two datasets differ by varying extents for individual chondrites, the $\delta^{41}K$ and $\delta^{87}Rb$ values correlate in both datasets (Fig. 3A). For example, the Murchison specimen analyzed at IPGP has both lower $\delta^{41}K$ and $\delta^{87}Rb$ values than the specimen reported by Nie et al. (2021). The correlation between $\delta^{41}K$ and $\delta^{87}Rb$ values suggests that the variability reflects isotopic heterogeneity at the analyzed sample scale. This isotopic heterogeneity could reflect different proportions of chondrules present in the two different specimens of a given chondrite. In this case, the specimen containing more chondrules should have a lower K abundance and a lower $\delta^{41}K$ value because chondrules are inferred to be depleted in K and its lighter isotope compared with the matrix, as indicated by the mixing curve in Fig. 3B. However, the specimen with the lower K abundance is often found to have a higher $\delta^{41}K$ value than that with the higher K abundance of the same chondrite (Fig. 3B), which is opposite to the expectation of mixing between varying proportions of chondrules with the matrix. Therefore, the observed sample heterogeneity cannot be due to the chondrule nugget effect alone but, to a greater extent, reflects the redistribution of K and its isotopes during aqueous alteration in chondrite parent bodies, which significantly altered the original K abundances and isotopic compositions in chondrules and matrix.

The effects of asteroidal aqueous alteration on the redistribution of alkalis in carbonaceous chondrites have been well documented, including the formation of diverse K-bearing phyllosilicate phases at < 100°C and/or anhydrous phases (e.g., nepheline and sodalite) due to Fe-alkali-halogen metasomatism at ~200°-300°C (e.g., Brearley, 2014; Ikeda and Kimura, 1996; Kimura and Ikeda, 1998; Krot et al., 1998; Krot et al., 1995). Ordinary chondrites also show signs, albeit more subtle, of interaction with aqueous fluids at varying temperatures, ranging

from low-temperature alteration (< 200°C, in the least-equilibrated petrologic type 3) to fluid-assisted metamorphism (200-400°C, in petrologic types of 4-6). Before or during the earliest stage of thermal metamorphism, aqueous fluids were suggested to have flowed through the fine-grained matrix, dissolving the mesostasis near the edge of chondrules and migrating alkalis into chondrule cores (e.g., Grossman et al., 2000; Grossman and Brearley, 2005). The presence of fluids is evidenced by the brine-bearing salt crystals found in the Monahans and Zag ordinary chondrites, which are argued to represent fluid samples from the early Solar System (Rubin et al., 2002; Zolensky et al., 1999). More recently, fluid activity on S-type asteroids is further supported by nanometer-sized halite crystals detected in particles returned from the asteroid Itokawa by JAXA's Hayabusa mission (Che and Zega, 2023). These observations collectively suggest the widespread action of fluids on primitive asteroids in the early Solar System.

Fluid-rock interactions have also been invoked to explain K isotopic variations in chondritic components of the Allende and Hamlet (LL4) chondrites (Jiang et al., 2021a; Koefoed et al., 2020). While inter-group variations in δ^{41}K are attributable to mixing between a CI-like matrix and K-poor, isotopically light chondrules, direct measurements on Allende and Hamlet show highly variable δ^{41}K in chondrules with values both higher and lower than those of the matrices (Fig. 3C and D). Furthermore, Ca-Al-inclusions (CAIs) formed well above the condensation temperature of K contain anomalously high K concentrations and δ^{41}K values. These observations are inconsistent with the low δ^{66}Zn and δ^{71}Ga values measured in CAIs interpreted as reflecting incomplete condensation (Kato et al., 2017; Luck et al., 2005). Instead of pristine nebular signatures, Jiang et al. (2021a) considered the high δ^{41}K values of CAIs as a secondary feature inherited from aqueous fluids assuming that most K in the CAIs was secondary in origin (Fig. 3C). Furthermore, they proposed that as the fluids interact with the porous matrix, the heavier K isotope was preferentially leached from the matrix and entered chondrules or CAIs, overprinting the original K abundances and isotopic signatures of the chondritic components.

The preference for the heavier K isotope by aqueous fluids is supported by the direction of K isotope fractionation during chemical weathering on Earth. Global rivers (−0.59‰ to 0.12‰) and oceans (0.12 ± 0.07‰, 2SD) have heavier K isotopic compositions (Hille et al., 2019; Li et al., 2019; Wang et al., 2020; Wang et al., 2021) than fresh basaltic rocks averaging at −0.42 ± 0.08‰ (2SD) (Hu et al., 2021; Tuller-Ross et al., 2019a; Tuller-Ross et al., 2019b). In addition, studies of weathering profiles and riverine sediments indicate that aqueous fluids preferentially

leach the heavy K isotope from the bedrock with apparent isotope fractionation factors of 0.08‰ to 0.55‰, leaving behind isotopically light weathered residues (down to −0.94‰, Chen et al., 2020; Li et al., 2019; Teng et al., 2020). Consistent with field analyses, theoretical calculations based on K-O bond strengths also suggest an enrichment of the heavier K isotope in aqueous solutions relative to typical silicate minerals and a fractionation factor of 0.24‰ between aqueous fluids and illite (Zeng et al., 2019).

At the onset of aqueous alteration, the K abundance and δ^{41}K value of matrix would have decreased, while the chondrules or CAIs would have increased K abundances and δ^{41}K values. With increasing degrees of alteration, chondrules, CAIs, and matrix would tend to approach equilibrium. The significant δ^{41}K variability in Allende and Murchison (Fig. 2) and the fact that the specimen with a lower K abundance often has a higher δ^{41}K value (Fig. 3B) suggest that these chondrites record early stages of aqueous alteration. A broad negative correlation between δ^{41}K values and K abundances is also observed in major groups of carbonaceous chondrites (Fig. S1), suggesting that aqueous alteration and associated redistribution of K isotopes occurred pervasively in the parent bodies of carbonaceous chondrites. Therefore, K isotopic variations in carbonaceous chondrites record volatility-driven isotope fractionations during chondrule formation, variable chondrule-matrix mixing at the accretion of chondrite parent bodies, and post-accretionary redistribution of K in chondrite parent bodies assisted by aqueous fluids.

4 Conclusions

Previous estimates of the K isotopic composition of the bulk Solar System were based heavily on CI chondrite Orgueil, whereas δ^{41}K values reported for two fragments of the CI-type specimen Ivuna show a large discrepancy. This study reports the K isotopic composition of the first samples returned from a carbonaceous asteroid (Ryugu) by JAXA's Hayabusa2 mission, thereby allowing for a direct comparison of CI chondrites with pristine asteroidal samples not contaminated by terrestrial environments. Analyses of three aliquots of Ryugu particles yield similar δ^{41}K values between −0.207‰ and −0.172‰. This range is consistent with the K isotopic compositions of most CI chondrites except for lower δ^{41}K values found in contaminated Orgueil samples and an anomalously low value previously reported for Ivuna. Based on the Ryugu samples and representative analyses of CI chondrites, we provide an updated estimate of the δ^{41}K

value for the bulk Solar System (−0.185 ± 0.078‰, 2SE). We suggest that samples of CI chondrites with $\delta^{41}K$ values significantly deviating from this range may reflect compositional heterogeneities due to aqueous alteration in CI parent bodies. Considerable K isotopic heterogeneity is also observed in other carbonaceous chondrites and within individual chondritic groups, whereby $\delta^{41}K$ values are broadly negatively correlated with K abundances. These observations suggest the widespread redistribution of K and its isotopes during aqueous alteration in chondrite parent bodies.

Acknowledgements

We appreciate the constructive comments from two anonymous reviewers that significantly improved the manuscript and Editor Alessandro Morbidelli for efficient handling the paper. We thank Julien Moureau and Tu-Han Luu for their assistance with mass spectrometer maintenance. This work was partly supported by the IPGP analytical platform PARI, Region Ile-de-France SESAME Grants no. 12015908, and DIM ACAV+, the ERC grant agreement No. 101001282 (METAL) (F.M.), the UnivEarthS Labex program (numbers: ANR-10-LABX-0023 and ANR-11-IDEX-0005-02) (F.M.), JSPS Kakenhi grants (S.T., H.Y., T.Y.), and the CNES.

All data referred to in this article can be found in the tables.

Tables

Table 1. Potassium abundance (ppm) and isotopic composition (‰) of Ryugu samples and carbonaceous chondrites analyzed in this study.

Sample	Group	δ^{41}K (‰)	2SD (‰)	95%c.i. (‰)	N	[K] (ppm)	Source	Treatment
Ryugu particles								
A0106		-0.150	0.065	0.060	4	436	Tokyo Tech	SOM, Zn,Fe,Ti,Cr chemistry
duplicate		-0.172	0.085	0.056	5			
repeat		-0.191	0.059	0.048	5			
Wtd average		-0.172	0.040	0.039				
C0107		-0.192	0.070	0.040	6	457	Tokyo Tech	SOM, Zn,Fe,Ti,Cr chemistry
duplicate		-0.214	0.066	0.056	5			
Wtd average		-0.204	0.030	0.048				
C0108		-0.188	0.086	0.059	5	604	Tokyo Tech	Zn,Fe,Ti,Cr chemistry
repeat		-0.220	0.072	0.069	4			
Wtd average		-0.207	0.045	0.055				
Ryugu average		-0.194	0.038					
Carbonaceous								
Orgueil	CI1	-0.081	0.070	0.066	5	568	IPGP	Powder dissolution
Tagish lake-1	C2-ung	-0.178	0.097	0.050	5	358	Tokyo Tech	Zn,Fe,Ti,Cr chemistry
duplicate		-0.181	0.057	0.048	5			
replicate		-0.215	0.057	0.043	6			Powder dissolution
Wtd average		-0.195	0.042	0.037				
Tagish lake-2		-0.201	0.042	0.023	8	360	IPGP	Powder dissolution
repeat		-0.236	0.051	0.030	7			
Wtd average		-0.215	0.049	0.032				
Tagish lake average		-0.205	0.029					
Tarda-1	C2-ung	-0.217	0.067	0.054	6	416	Tokyo Tech	Zn,Fe,Ti,Cr chemistry
duplicate		-0.230	0.076	0.037	4			
repeat		-0.224	0.056	0.045	5			
Wtd average		-0.223	0.013	0.037				
Tarda-2		-0.166	0.063	0.050	5	416	IPGP	Powder dissolution
repeat		-0.222	0.054	0.047	5			
repeat		-0.218	0.058	0.039	4			
replicate		-0.204	0.056	0.038	7			Powder dissolution
duplicate		-0.189	0.060	0.047	6			
repeat		-0.222	0.060	0.050	5			
Wtd average		-0.205	0.044	0.024				
Tarda average		-0.214	0.026					
Murchison	CM2	-0.250	0.049	0.043	7	411	IPGP	Powder dissolution
Cold Bokkeveld	CM2	-0.267	0.064	0.035	7	476	IPGP	Powder dissolution
Lancé	CO3.5	-0.382	0.087	0.040	7	430	IPGP	Powder dissolution
Allende (A)-1	CV3	-0.293	0.056	0.052	5	296	Tokyo Tech	Zn,Fe,Ti,Cr chemistry
repeat		-0.292	0.072	0.048	5			
Wtd average		-0.292	0.001	0.044				
Allende-2		-0.151	0.062	0.059	5	267	IPGP	Powder dissolution
repeat		-0.181	0.062	0.055	4			
repeat		-0.168	0.052	0.045	6			
replicate		-0.178	0.065	0.031	4			Powder dissolution
Wtd average		-0.169	0.027	0.030				

Note: 'repeat' indicates repeat instrumental analysis. 'duplicate' indicate repeat column chemistry and instrumental analysis. 'replicate' indicates repeat sample dissolution, column chemistry, and instrumental analysis. The number '-1' and '-2' attached to the same names indicate different pieces of a given chondrite. 'SOM' is short for 'Soluble Organic Matter extraction.'

491 **Table S1**. Potassium isotopic compositions (‰) of terrestrial samples analyzed in this study.

Geostandard	Description	$\delta^{41}K$ (‰)	2SD (‰)	95% c.i. (‰)	N
BIR	Basalt	-0.448	0.059	0.036	7
replicate		-0.400	0.052	0.076	4
repeat		-0.414	0.050	0.062	4
Wtd average		-0.418	0.050	0.031	
BCR-2	Basalt	-0.404	0.051	0.019	8
repeat		-0.443	0.044	0.024	7
replicate		-0.425	0.066	0.034	5
Wtd average		-0.426	0.039	0.030	
AGV-2	Andesite	-0.455	0.042	0.030	7
Pacific seawater		0.152	0.060	0.054	4
repeat		0.128	0.078	0.050	6
repeat		0.113	0.039	0.037	7
repeat		0.133	0.084	0.056	5
Wtd average		0.126	0.032	0.028	

492

Figures

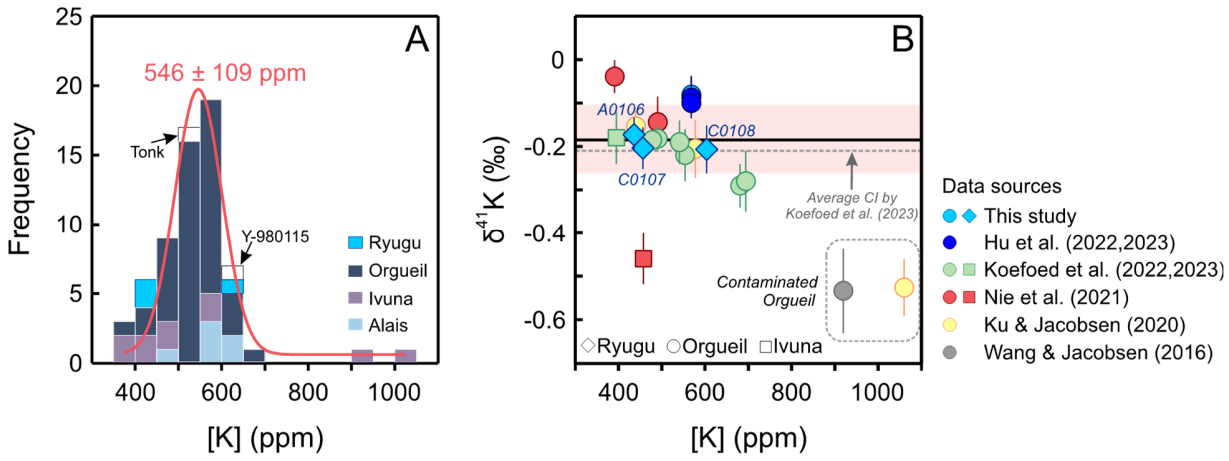

Figure 1. Potassium abundances ([K], ppm) and isotope compositions (δ^{41}K, ‰) of CI chondrites and Ryugu samples. (A) A histogram of K abundances in CI chondrites reported in the literature (Ahrens et al., 1969; Anders and Grevesse, 1989; Barrat et al., 2012; Beer et al., 1984; Braukmüller et al., 2018; Edwards and Urey, 1955; Jarosewich, 1990; Kallemeyn and Wasson, 1981; Kaushal and Wetherill, 1970; Makishima and Nakamura, 2006; Mittlefehldt, 2002; Nakamura, 1974; Nichiporuk and Moore, 1974; Palme and Zipfel, 2022; Von Michaelis et al., 1969; Wiik, 1956). (B) The three aliquots of Ryugu particles have indistinguishable δ^{41}K values and fall within the range of CI chondrites except for an anomalously lower δ^{41}K value previously reported for Ivuna. The horizontal black line and pink field indicate the average δ^{41}K value of Ryugu samples and CI chondrites (−0.185 ± 0.078‰), representing the current best estimate of the bulk K isotopic composition of the Solar System. The dashed grey line is the average CI chondrites reported by Koefoed et al. (2023) and is plotted for comparison. Crustal contamination results in elevated K abundances and crust-like, lower δ^{41}K compared with pristine CI chondrite values (Ku and Jacobsen, 2020; Wang and Jacobsen, 2016). The K abundance of Ryugu C0108 is from Yokoyama et al. (2022), while those of A0106 and C0107 are new data reported in this study (Table 1).

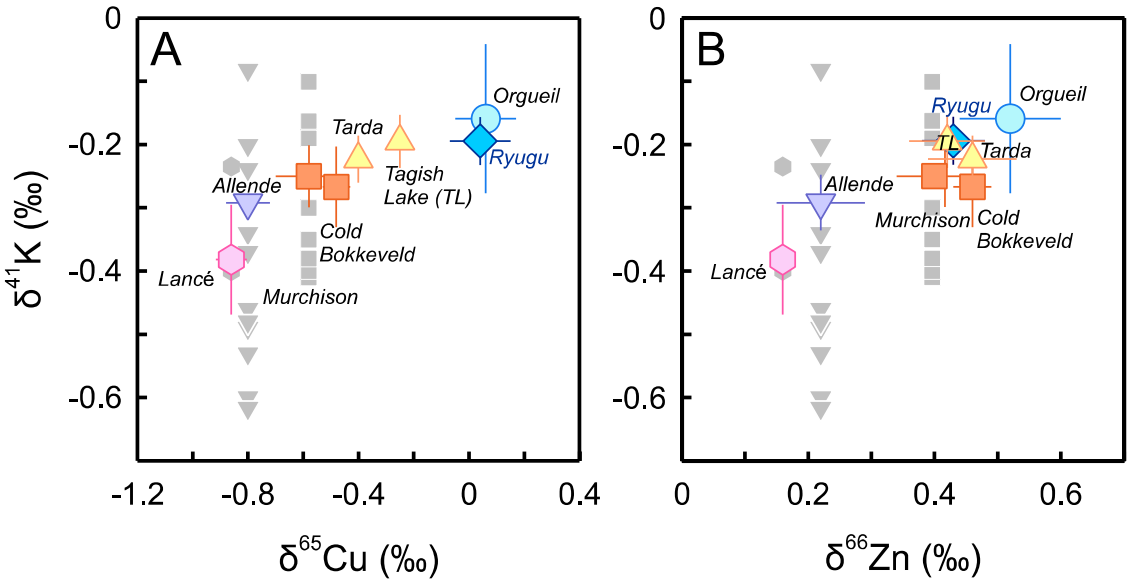

512

513 **Figure 2.** Positive correlations of $\delta^{41}K$ values with (A) $\delta^{65}Cu$ values and (B) $\delta^{66}Zn$ values in
514 Ryugu samples and different groups of carbonaceous chondrites. These correlations suggest
515 inter-group variations in $\delta^{41}K$ primarily reflect mixing of a CI-, or Ryugu-like matrix component
516 with the heaviest isotopic compositions and a volatile-depleted refractory component such as
517 chondrules carrying the light isotopic signatures. The colored symbols are data from this study
518 and the grey symbols are literature values. In (A), $\delta^{41}K$ and $\delta^{65}Cu$ values (Paquet et al., 2022) for
519 Ryugu, Tarda, Allende were measured from the same specimens. $\delta^{65}Cu$ values for Orgueil and
520 Murchison are from Paquet et al. (2022), for Tagish Lake, Cold Bokkeveld, and Lancé are from
521 Luck et al. (2003). In (B), $\delta^{41}K$ and $\delta^{66}Zn$ values (Paquet et al., 2022; Pringle et al., 2017) for
522 Ryugu, Tagish Lake, Tarda, Murchison, Cold Bokkeveld, Lancé, and Allende were measured
523 from the same specimens. $\delta^{66}Zn$ value for Orgueil is from Paquet et al. (2022). Literature $\delta^{41}K$
524 values are from Bloom et al. (2020); Jiang et al. (2021a); Jiang et al. (2021b); Koefoed et al.
525 (2023); Koefoed et al. (2022); Ku and Jacobsen (2020); Nie et al. (2021). Although literature
526 $\delta^{41}K$ values were plotted with $\delta^{65}Cu$ and $\delta^{66}Zn$ values measured from different specimens of a
527 given chondrite, $\delta^{65}Cu$ and $\delta^{66}Zn$ values reported for different specimens of Orgueil, Murchison,
528 and Allende generally agree well (Barrat et al., 2012; Luck et al., 2005; Luck et al., 2003; Paquet
529 et al., 2022; Pringle et al., 2017).

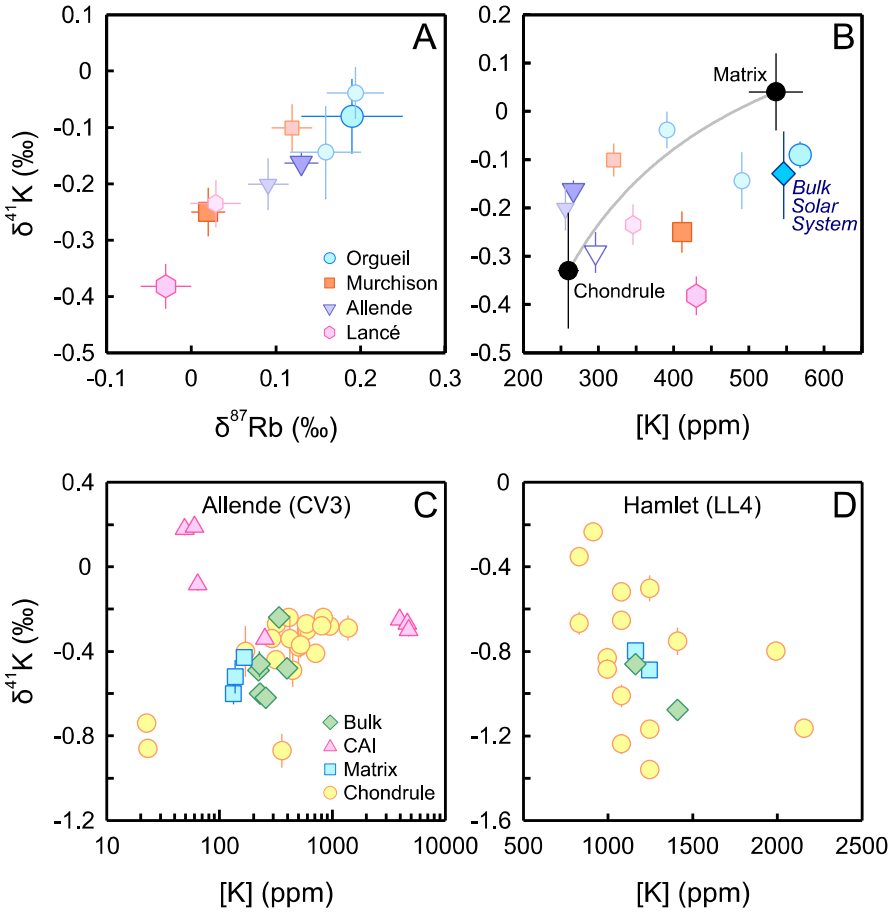

530

531 **Figure 3.** K isotopic evidence of aqueous alteration of chondrites in their parent bodies. (A)
532 Positively correlated $\delta^{41}K$ and $\delta^{87}Rb$ values indicate sample heterogeneity for a given chondrite.
533 The larger symbols are data from this study and the smaller symbols are from Nie et al. (2021).
534 (B) The broad positive correlation between $\delta^{41}K$ values and K abundances across different
535 carbonaceous chondrite groups indicates mixing of the CI-like, isotopically heavy matrix with K-
536 depleted, isotopically light chondrules, as indicated by the mixing curve using endmember
537 compositions extrapolated in Nie et al. (2021). However, for a given chondrite (coded with the
538 same color), the specimen with the higher K abundance often has a lower $\delta^{41}K$ value than that
539 with the lower K abundance. The large solid triangle down is an Allende specimen from IPGP,
540 and the open triangle down is an aliquot of pulverized Allende provided by the Smithsonian
541 Museum. The blue diamond symbol indicates the new estimate of the composition of the bulk
542 Solar System from this study. (C) and (D) $\delta^{41}K$ values measured in chondrules, calcium-
543 aluminum-rich inclusions (CAIs), and matrices in Allende and Hamlet chondrites show
544 significant alteration of the original K abundances and $\delta^{41}K$ values of all chondritic components.
545 Data source: Data presented in (A) and (B) are from this study and the literature (Nie et al., 2021;
546 Pringle and Moynier, 2017), whereas those presented in (C) and (D) are from Jiang et al.
547 (2021a); Ku et al. (2022), and Koefoed et al. (2020).

References

Ahrens, L. H., Von Michaelis, H., Fesq, H. W., 1969. The composition of the stony meteorites (IV) some analytical data on Orgueil, Nogoya, Ornans and Ngawi. Earth and Planetary Science Letters. 6**,** 285-288.

Alexander, C. M. O. D., 2005. Re-examining the role of chondrules in producing the elemental fractionations in chondrites. Meteoritics & Planetary Science. 40**,** 943-965.

Anders, E., Grevesse, N., 1989. Abundances of the elements: Meteoritic and solar. Geochimica et Cosmochimica Acta. 53**,** 197-214.

Arakawa, M., et al., 2020. An artificial impact on the asteroid (162173) Ryugu formed a crater in the gravity-dominated regime. Science. 368**,** 67-71.

Barrat, J. A., Zanda, B., Moynier, F., Bollinger, C., Liorzou, C., Bayon, G., 2012. Geochemistry of CI chondrites: Major and trace elements, and Cu and Zn Isotopes. Geochimica et Cosmochimica Acta. 83**,** 79-92.

Beer, H., Walter, G., Macklin, R. L., Patchett, P. J., 1984. Neutron capture cross sections and solar abundances of 160,161Dy, 170,171Yb, 175,176Lu, and 176,177Hf for the s-process analysis of the radionuclide 176Lu. Physical Review C. 30**,** 464-478.

Bloom, H., et al., 2020. Potassium isotope compositions of carbonaceous and ordinary chondrites: Implications on the origin of volatile depletion in the early solar system. Geochimica et Cosmochimica Acta. 277**,** 111-131.

Braukmüller, N., Wombacher, F., Hezel, D. C., Escoube, R., Münker, C., 2018. The chemical composition of carbonaceous chondrites: Implications for volatile element depletion, complementarity and alteration. Geochimica et Cosmochimica Acta. 239**,** 17-48.

Brearley, A. J., 2006. The action of water. Meteorites and the early solar system II. 943**,** 587-624.

Brearley, A. J., 2014 1.9 - Nebular Versus Parent Body Processing. In: H. D. Holland, K. K. Turekian, (Eds.), Treatise on Geochemistry (Second Edition). Elsevier, Oxford, pp. 309-334.

Che, S., Zega, T. J., 2023. Hydrothermal fluid activity on asteroid Itokawa. Nature Astronomy.

Chen, H., Liu, X.-M., Wang, K., 2020. Potassium isotope fractionation during chemical weathering of basalts. Earth and Planetary Science Letters. 539**,** 116192.

Chen, H., Tian, Z., Tuller-Ross, B., Korotev, Randy L., Wang, K., 2019. High-precision potassium isotopic analysis by MC-ICP-MS: an inter-laboratory comparison and refined K atomic weight. Journal of Analytical Atomic Spectrometry. 34**,** 160-171.

Clayton, R. N., 1993. Oxygen Isotopes in Meteorites. Annual Review of Earth and Planetary Sciences. 21**,** 115-149.

Edwards, G., Urey, H. C., 1955. Determination of alkali metals in meteorites by a distillation process. Geochimica et Cosmochimica Acta. 7**,** 154-168.

Grossman, J. N., ALEXANDER, C. M. O. D., Wang, J., Brearley, A. J., 2000. Bleached chondrules: Evidence for widespread aqueous processes on the parent asteroids of ordinary chondrites. Meteoritics & Planetary Science. 35**,** 467-486.

Grossman, J. N., Brearley, A. J., 2005. The onset of metamorphism in ordinary and carbonaceous chondrites. Meteoritics & Planetary Science. 40**,** 87-122.

Hille, M., Hu, Y., Huang, T.-Y., Teng, F.-Z., 2019. Homogeneous and heavy potassium isotopic composition of global oceans. Science Bulletin. 64**,** 1740-1742.

Hopp, T., et al., 2022. Ryugu's nucleosynthetic heritage from the outskirts of the Solar System. Science Advances. 8**,** eadd8141.

Hu, Y., Chen, X.-Y., Xu, Y.-K., Teng, F.-Z., 2018. High-precision analysis of potassium isotopes by HR-MC-ICPMS. Chemical Geology. 493**,** 100-108.

Hu, Y., Moynier, F., Bizzarro, M., 2022. Potassium isotope heterogeneity in the early Solar System controlled by extensive evaporation and partial recondensation. Nature Communications. 13**,** 7669.

Hu, Y., Moynier, F., Yang, X., 2023. Volatile-depletion processing of the building blocks of Earth and Mars as recorded by potassium isotopes. Earth and Planetary Science Letters. 620**,** 118319.
Hu, Y., Teng, F.-Z., Helz, R. T., Chauvel, C., 2021. Potassium isotope fractionation during magmatic differentiation and the composition of the mantle. Journal of Geophysical Research: Solid Earth. 126**,** e2020JB021543.
Ikeda, Y., Kimura, M., 1996. Anhydrous alteration of Allende chondrules in the solar nebula III: Alkali-zoned chondrules and heating experiments for anhydrous alteration. Antarctic Meteorite Research. 9**,** 51.
Jarosewich, E., 1990. Chemical analyses of meteorites: A compilation of stony and iron meteorite analyses. Meteoritics. 25**,** 323-337.
Jiang, Y., et al., 2021a. Early solar system aqueous activity: K isotope evidence from Allende. Meteoritics & Planetary Science. 56**,** 61-76.
Jiang, Y., Koefoed, P., Wang, K., Xu, W.-B., 2021b. High precision potassium isotopic study of Chinese Antarctic chondrites. Acta Geologica Sinica. 95.
Kallemeyn, G. W., Wasson, J. T., 1981. The compositional classification of chondrites—I. The carbonaceous chondrite groups. Geochimica et Cosmochimica Acta. 45**,** 1217-1230.
Kato, C., Moynier, F., Foriel, J., Teng, F.-Z., Puchtel, I. S., 2017. The gallium isotopic composition of the bulk silicate Earth. Chemical Geology. 448**,** 164-172.
Kaushal, S. K., Wetherill, G. W., 1970. Rubidium 87-Strontium 87 age of carbonaceous chondrites. Journal of Geophysical Research (1896-1977). 75**,** 463-468.
Kimura, M., Ikeda, Y., 1998. Hydrous and anhydrous alterations of chondrules in Kaba and Mokoia CV chondrites. Meteoritics & Planetary Science. 33**,** 1139-1146.
Kitazato, K., et al., 2019. The surface composition of asteroid 162173 Ryugu from Hayabusa2 near-infrared spectroscopy. Science. 364**,** 272-275.
Koefoed, P., et al., 2023. The potassium isotopic composition of CI chondrites and the origin of isotopic variations among primitive planetary bodies. Geochimica et Cosmochimica Acta.
Koefoed, P., Pravdivtseva, O., Chen, H., Gerritzen, C., Thiemens, M. M., Wang, K., 2020. Potassium isotope systematics of the LL4 chondrite Hamlet: Implications for chondrule formation and alteration. Meteoritics & Planetary Science. 55.
Koefoed, P., et al., 2022. The dynamic formation process of the CB chondrite Gujba. Geochimica et Cosmochimica Acta. 332**,** 33-56.
Krot, A. N., Petaev, M. I., Scott, E. R. D., Choi, B.-G., Zolensky, M. E., Keil, K., 1998. Progressive alteration in CV3 chondrites: More evidence for asteroidal alteration. Meteoritics & Planetary Science. 33**,** 1065-1085.
Krot, A. N., Scott, E. R. D., Zolensky, M. E., 1995. Mineralogical and chemical modification of components in CV3 chondrites: Nebular or asteroidal processing? Meteoritics. 30**,** 748-775.
Ku, Y., Jacobsen, S. B., 2020. Potassium isotope anomalies in meteorites inherited from the protosolar molecular cloud. Science Advances. 6**,** eabd0511.
Ku, Y., Petaev, M. I., Jacobsen, S. B., 2022. The Timing of Potential Last Nucleosynthetic Injections into the Protosolar Molecular Cloud Inferred from ⁴¹Ca–²⁶Al Systematics of Bulk CAIs. The Astrophysical Journal Letters. 931**,** L13.
Li, S., et al., 2019. K isotopes as a tracer for continental weathering and geological K cycling. Proceedings of the National Academy of Sciences. 116**,** 8740-8745.
Luck, J.-M., Othman, D. B., Albarède, F., 2005. Zn and Cu isotopic variations in chondrites and iron meteorites: Early solar nebula reservoirs and parent-body processes. Geochimica et Cosmochimica Acta. 69**,** 5351-5363.
Luck, J. M., Othman, D. B., Barrat, J. A., Albarède, F., 2003. Coupled 63Cu and 16O excesses in chondrites. Geochimica et Cosmochimica Acta. 67**,** 143-151.

Makishima, A., Nakamura, E., 2006. Determination of major/minor and trace elements in silicate samples by ICP-QMS and ICP-SFMS applying isotope dilution-internal standardisation (ID-IS) and multi-stage internal standardisation. Geostandards and Geoanalytical Research. 30**,** 245-271.

McSween, H. Y., Ghosh, A., Grimm, R. E., Wilson, L., Young, E. D., 2002. Thermal evolution models of asteroids. Asteroids III. 559**,** 559-572.

Mittlefehldt, D. W., 2002. Geochemistry of the ungrouped carbonaceous chondrite Tagish Lake, the anomalous CM chondrite Bells, and comparison with CI and CM chondrites. Meteoritics & Planetary Science. 37**,** 703-712.

Morlok, A., Bischoff, A., Stephan, T., Floss, C., Zinner, E., Jessberger, E. K., 2006. Brecciation and chemical heterogeneities of CI chondrites. Geochimica et Cosmochimica Acta. 70**,** 5371-5394.

Morota, T., et al., 2020. Sample collection from asteroid (162173) Ryugu by Hayabusa2: Implications for surface evolution. Science. 368**,** 654-659.

Moynier, F., et al., 2022. The Solar System calcium isotopic composition inferred from Ryugu samples. Geochemical Perspectives Letters. 24**,** 1-6.

Moynier, F., et al., 2021. Potassium isotopic composition of various samples using a dual-path collision cell-capable multiple-collector inductively coupled plasma mass spectrometer, Nu instruments Sapphire. Chemical Geology. 571**,** 120144.

Nakamura, E., et al., 2022. On the origin and evolution of the asteroid Ryugu: A comprehensive geochemical perspective. Proceedings of the Japan Academy, Series B. 98**,** 227-282.

Nakamura, N., 1974. Determination of REE, Ba, Fe, Mg, Na and K in carbonaceous and ordinary chondrites. Geochimica et Cosmochimica Acta. 38**,** 757-775.

Naraoka, H., et al., 2023. Soluble organic molecules in samples of the carbonaceous asteroid (162173) Ryugu. Science. 379**,** eabn9033.

Nichiporuk, W., Moore, C. B., 1974. Lithium, sodium and potassium abundances in carbonaceous chondrites. Geochimica et Cosmochimica Acta. 38**,** 1691-1701.

Nie, N. X., et al., 2021. Imprint of chondrule formation on the K and Rb isotopic compositions of carbonaceous meteorites. Science Advances. 7**,** eabl3929.

Palme, H., Lodders, K., Jones, A., 2014 2.2 - Solar System abundances of the elements. In: H. D. Holland, K. K. Turekian, (Eds.), Treatise on Geochemistry (Second Edition). Elsevier, Oxford, pp. 15-36.

Palme, H., Zipfel, J., 2022. The composition of CI chondrites and their contents of chlorine and bromine: Results from instrumental neutron activation analysis. Meteoritics & Planetary Science. 57**,** 317-333.

Paquet, M., et al., 2022. Contribution of Ryugu-like material to Earth's volatile inventory by Cu and Zn isotopic analysis. Nature Astronomy.

Pilorget, C., et al., 2022. First compositional analysis of Ryugu samples by the MicrOmega hyperspectral microscope. Nature Astronomy. 6**,** 221-225.

Pringle, E. A., Moynier, F., 2017. Rubidium isotopic composition of the Earth, meteorites, and the Moon: Evidence for the origin of volatile loss during planetary accretion. Earth and Planetary Science Letters. 473**,** 62-70.

Pringle, E. A., Moynier, F., Beck, P., Paniello, R., Hezel, D. C., 2017. The origin of volatile element depletion in early solar system material: Clues from Zn isotopes in chondrules. Earth and Planetary Science Letters. 468**,** 62-71.

Rubin, A. E., 2012. Collisional facilitation of aqueous alteration of CM and CV carbonaceous chondrites. Geochimica et Cosmochimica Acta. 90**,** 181-194.

Rubin, A. E., Zolensky, M. E., Bodnar, R. J., 2002. The halite-bearing Zag and Monahans (1998) meteorite breccias: Shock metamorphism, thermal metamorphism and aqueous alteration on the H-chondrite parent body. Meteoritics & Planetary Science. 37**,** 125-141.

Sugita, S., et al., 2019. The geomorphology, color, and thermal properties of Ryugu: Implications for parent-body processes. Science. 364**,** eaaw0422.
Tachibana, S., et al., 2022. Pebbles and sand on asteroid (162173) Ryugu: In situ observation and particles returned to Earth. Science. 375**,** 1011-1016.
Teng, F.-Z., Hu, Y., Ma, J.-L., Wei, G.-J., Rudnick, R. L., 2020. Potassium isotope fractionation during continental weathering and implications for global K isotopic balance. Geochimica et Cosmochimica Acta. 278**,** 261-271.
Tomeoka, K., Buseck, P. R., 1988. Matrix mineralogy of the Orgueil CI carbonaceous chondrite. Geochimica et Cosmochimica Acta. 52**,** 1627-1640.
Tuller-Ross, B., Marty, B., Chen, H., Kelley, K. A., Lee, H., Wang, K., 2019a. Potassium isotope systematics of oceanic basalts. Geochimica et Cosmochimica Acta. 259**,** 144-154.
Tuller-Ross, B., Savage, P. S., Chen, H., Wang, K., 2019b. Potassium isotope fractionation during magmatic differentiation of basalt to rhyolite. Chemical Geology. 525**,** 37-45.
Von Michaelis, H., Ahrens, L. H., Willis, J. P., 1969. The composition of stony meteorites. II. The analytical data and an assessment of their quality. Earth and Planetary Science Letters. 5**,** 387-394.
Wang, K., Close, H. G., Tuller-Ross, B., Chen, H., 2020. Global Average Potassium Isotope Composition of Modern Seawater. ACS Earth and Space Chemistry. 4**,** 1010-1017.
Wang, K., Jacobsen, S. B., 2016. Potassium isotopic evidence for a high-energy giant impact origin of the Moon. Nature. 538**,** 487-490.
Wang, K., Peucker-Ehrenbrink, B., Chen, H., Lee, H., Hasenmueller, E. A., 2021. Dissolved potassium isotopic composition of major world rivers. Geochimica et Cosmochimica Acta. 294**,** 145-159.
Wiik, H. B., 1956. The chemical composition of some stony meteorites. Geochimica et Cosmochimica Acta. 9**,** 279-289.
Xu, Y.-K., et al., 2019. Potassium isotopic compositions of international geological reference materials. Chemical Geology. 513**,** 101-107.
Yada, T., et al., 2022. Preliminary analysis of the Hayabusa2 samples returned from C-type asteroid Ryugu. Nature Astronomy. 6**,** 214-220.
Yokoyama, T., et al., 2022. Samples returned from the asteroid Ryugu are similar to Ivuna-type carbonaceous meteorites. Science. 0**,** eabn7850.
Zeng, H., et al., 2019. Ab Initio Calculation of Equilibrium Isotopic Fractionations of Potassium and Rubidium in Minerals and Water. ACS Earth and Space Chemistry. 3**,** 2601-2612.
Zolensky, M., McSween, H. Y., 1988 Aqueous alteration. In: J. F. Kerridge, M. S. Matthews, (Eds.), Meteorites and the Early Solar System, pp. 114-143.
Zolensky, M. E., et al., 1999. Asteroidal water within fluid inclusion-bearing halite in an H5 chondrite, Monahans (1998). Science. 285**,** 1377-1379.

Declaration of interests

The authors declare that they have no known competing financial interests or personal relationships that could have appeared to influence the work reported in this paper.